Involvement of *Neurospora* Mitochondrial Tyrosyl-tRNA Synthetase in RNA Splicing. A New Method for Purifying the Protein and Characterization of Physical and Enzymatic Properties Pertinent to Splicing†

Roland J. Saldanha,‡ Smita S. Patel,‡ Rajendran Surendran,§ James C. Lee,§ and Alan M. Lambowitz*,‡

Departments of Molecular Genetics, Biochemistry, and Medical Biochemistry, The Ohio State University, 484 West Twelfth Avenue, Columbus, Ohio 43210-1292, and Department of Human Biological Chemistry and Genetics, The University of Texas Medical Branch, Galveston, Texas 77555-1055

Received July 26, 1994; Revised Manuscript Received October 5, 1994⊗

ABSTRACT: The *Neurospora* CYT-18 protein, the mitochondrial tyrosyl-tRNA synthetase, functions in the splicing of group I introns. Here, bacterially expressed CYT-18 protein, purified by a new procedure involving polyethyleneimine precipitation to remove tightly bound nucleic acids, was used to characterize properties pertinent to RNA splicing. Analytical ultracentrifugation and other methods showed that the CYT-18 protein is an asymmetric homodimer. The measured frictional ratio, f/f_o=1.55, corresponds to an axial ratio of 10 for a prolate ellipsoid or 12 for an oblate ellipsoid. Like bacterial TyrRSs, the CYT-18 protein exhibits half-sites reactivity, each homodimer having one active site for tyrosyl adenylation and RNA splicing. The splicing activity of CYT-18 was unaffected by aminoacylation substrates at concentrations used in aminoacylation reactions, whereas the TyrRS activity was inhibited by physiological concentrations of the splicing cofactor GTP, as well as CTP or UTP, or by low concentrations of a group I intron RNA. Kinetic measurements suggest that the binding of CYT-18 to a group I intron substrate is a two-step process, with an initial bimolecular step that is close to diffusion limited ($3.24 \pm 0.03 \times 10^7$ M^{-1} s^{-1}) followed by a slower conformational change (0.54 ± 0.07 s^{-1}). After CYT-18 binding, splicing occurs at a rate of 0.0025 s^{-1}, within 6-fold of the rate of self-splicing of the *Tetrahymena* large rRNA intron *in vitro*. The K_d for the complex between the CYT-18 protein and a group I intron substrate, calculated from k_{off}/k_{on}, was <0.3 pM, substantially lower than determined by presumed equilibrium measurements [Guo, Q., & Lambowitz, A. M. (1992) *Genes Dev. 6*, 1357−1372]. As a result of this tight binding, the CYT-18 protein functions stoichiometrically in *in vitro* splicing reactions due to its extremely slow dissociation from the excised intron RNA. The very tight binding of the CYT-18 protein to the intron RNA raises the possibility that specific mechanisms exist for dissociating the protein from the excised intron *in vivo*.

The *Neurospora* mitochondrial tyrosyl-tRNA synthetase (mt TyrRS),[1] which is encoded by the nuclear gene *cyt-18*, functions in the splicing of the mt large rRNA intron and other group I introns in *Neurospora* mitochondria (Collins & Lambowitz, 1985; Akins & Lambowitz, 1987). The CYT-18-dependent splicing of group I introns occurs by the same guanosine-initiated transesterification reaction used by self-splicing group I introns (Garriga & Lambowitz, 1983, 1986). The splicing reactions remain essentially RNA catalyzed, and the protein functions by facilitating the correct folding of the precursor RNA (Guo et al., 1991; Guo & Lambowitz, 1992; Mohr et al., 1992). Although additional components may be required for efficient splicing *in vivo*, purified CYT-18 protein isolated from mitochondria or synthesized via an expression plasmid in *Escherichia coli* is by itself sufficient to splice the *Neurospora* mt large rRNA intron *in vitro* (Majumder et al., 1989; Kittle et al., 1991). The purified CYT-18 protein also binds group I introns from yeast, other fungi, and bacteriophage (Guo & Lambowitz, 1992), and the CYT-18 protein expressed in *E. coli* can restore the splicing of mutants of the phage T4 *td* intron *in vivo* (Mohr et al., 1992). The ability of CYT-18 to splice diverse group I introns indicates that it recognizes highly conserved structural features of these introns.

The group I intron catalytic core is believed to consist of two extended helices, one formed by the coaxial stacking of the secondary structure elements P5, P4, P6, and P6a and the other by the stacking of P3, P8, and P7, with the two helices creating a cleft that contains the intron's active site (Kim & Cech, 1987; Michel & Westhof, 1990). Nitrocellulose filter binding experiments showed that CYT-18 binds with high affinity to a small RNA containing the P4−P5−P6−P6a segment of the *Neurospora* mt large rRNA intron, but that additional sequences, including P7−P9 on the other helix, are required for maximal binding (Guo & Lambowitz,

† This work was supported by NIH Grant GM37951 to A.M.L. The analytical ultracentrifugation experiments were supported by Grants H-0013 and H-1238 from the R. A. Welch Foundation to J.C.L.

* Address correspondence to this author at Department of Molecular Genetics, The Ohio State University, 484 W. Twelfth Ave., Columbus, OH 43210-1292. Phone: (614) 292-5606. Fax: (614) 292-4466.

‡ The Ohio State University.

§ The University of Texas Medical Branch.

⊗ Abstract published in *Advance ACS Abstracts,* January 1, 1995.

[1] Abbreviations: bp, base pair; DTT, dithiothreitol; kb, kilobase(s); MOPS, 3-(*N*-morpholino)propanesulfonic acid; mt, mitochondrial; nt, nucleotide; ORF, open reading frame; PEI, polyethyleneimine; phenol-CIA, phenol−chloroform−isoamyl alcohol (25:24:1); PMSF, phenylmethanesulfonyl fluoride; RNP, ribonucleoprotein; td, thymidylate synthetase; TyrRS, tyrosyl-tRNA synthetase.

0006-2960/95/0434-1275$09.00/0

1992). These findings, together with the ability of CYT-18 to compensate for structural defects in different regions of the group I intron catalytic core, suggest that the CYT-18 protein functions in splicing by binding to each of the two major helices of the catalytic core and stabilizing them in the correct relative orientation to form the intron's active site (Guo & Lambowitz, 1992; Mohr et al., 1992).

The CYT-18 protein is homologous to well-studied bacterial TyrRSs, as well as to the yeast and *Podospora anserina* mt TyrRS (Kämper et al., 1992). However, only the *Neurospora* and *Podospora* TyrRSs are capable of splicing group I introns, presumably reflecting some adaptation of the basic protein structure that confers splicing activity (Cherniack et al., 1990; Kämper et al., 1992). The bacterial TyrRSs consist of an N-terminal nucleotide-binding-fold region, which catalyzes tyrosyl adenylation and binds the acceptor stem of the tRNA, followed by a C-terminal domain, which binds other regions of the tRNA (Carter et al., 1986; Bedouelle & Winter, 1986). CYT-18's nucleotide-binding-fold region is relatively well conserved compared to bacterial TyrRSs, whereas the putative C-terminal tRNA-binding domain has diverged to a greater extent (Akins & Lambowitz, 1987; Cherniack et al., 1990; Kittle et al., 1991). Analysis of *in vivo* and *in vitro* mutants showed that regions of CYT-18 required for splicing include a small, idiosyncratic N-terminal domain that is not present in bacterial TyrRSs, the C-terminal tRNA-binding domain, and probably parts of the nucleotide-binding fold region (Cherniack et al., 1990; Kittle et al., 1991). The regions required for splicing overlap those required for TyrRS activity, and both activities are inhibited in parallel by small linker-insertion mutations in the C-terminal tRNA-binding domain, suggesting that some similar interactions with this region are involved in binding both the intron and tRNA substrates (Kittle et al., 1991). Further, a group I intron RNA was found to be a competitive inhibitor of aminoacylation, providing direct evidence that it competes with $tRNA^{Tyr}$ for the same or an overlapping binding site (Guo & Lambowitz, 1992).

Notably, the bacterial TyrRSs have been shown to function as homodimers exhibiting half-sites reactivity. Each homodimer binds only one molecule of tyrosine, ATP, and $tRNA^{Tyr}$ and forms one molecule of tyrosyl adenylate (Fersht, 1975; Jakes & Fersht, 1975; Dessen et al., 1982). The $tRNA^{Tyr}$ binds asymmetrically across the surface of the two subunits of the homodimer, interacting with the N-terminal region of one subunit and the C-terminal region of the other (Bedouelle & Winter, 1986; Carter et al., 1986; Bedouelle, 1990). Similarly for the CYT-18 protein, nitrocellulose filter binding experiments indicated that one molecule of intron RNA is bound per two monomer units (Guo & Lambowitz, 1992). Gel filtration of CYT-18 protein from micrococcal nuclease-digested mt RNP particles showed that both TyrRS and RNA splicing activity coeluted with a peak of CYT-18 at approximately the position expected for a homodimer (Majumder et al., 1989). However, the mt RNP particle preparations were impure, some splicing activity trailed the major peak, and a substantial amount of inactive CYT-18 protein eluted at higher apparent molecular weights, possibly reflecting the presence of larger complexes or aggregation.

The dual function of the CYT-18 protein raises the possibility that mechanisms exist to regulate whether it has splicing or TyrRS activity. Such mechanisms might include the binding of substrates or cofactors of the aminoacylation or splicing reactions, the binding of other small molecules, covalent modification of the protein, or changes in quaternary structure. Two-dimensional isoelectric focusing/SDS−polyacrylamide gel electrophoresis failed to detect covalently modified forms of the CYT-18 protein in *Neurospora* mitochondria (Majumder et al., 1989). Although two distinct peaks of CYT-18 were resolved by phosphocellulose or heparin-Sepharose chromatography (Akins & Lambowitz, 1987; Majumder et al., 1989; Kittle et al., 1991), it remained possible that the chromatographic separation merely reflected the incomplete removal of nucleic acids that were tightly bound to some proportion of the protein.

Recently, we developed methods for synthesizing active CYT-18 protein in *E. coli*, thereby circumventing some of the difficulties in studying the protein from mitochondria. In the present work, we devised a new procedure for purifying highly active, bacterially expressed CYT-18 protein by using PEI precipitation to remove tightly bound nucleic acids. This procedure gives CYT-18 protein that elutes from carboxymethyl-Sepharose columns as a single peak of 90−95% pure protein, with a yield of 30−50 mg/L of culture. These relatively pure preparations of the CYT-18 protein were used to study its physical and enzymatic properties and its possible regulation by substrates of the TyrRS and splicing reactions.

MATERIALS AND METHODS

Recombinant Plasmids. pEX560 (previously designated pEX550A) was used for expression of CYT-18 protein in *E. coli* (Kittle et al., 1991). This plasmid is a pET3a derivative (Rosenberg et al., 1987) that contains a 638 amino acid *cyt-18* ORF inserted downstream of the phage T7 promoter. The ORF lacks the N-terminal mitochondrial targeting sequence but has an additional N-terminal AUG codon for expression in *E. coli.*

pBD5a contains a 388 nt-derivative of the mt large rRNA intron plus flanking exons cloned downstream of the phage T3 promoter in pBS(+) (Guo et al., 1991). Linearization of pBD5a with *Ban*I and transcription with phage T3 RNA polymerase yields a 503 nt transcript containing a 65 nt 5′ exon, 388 nt intron, and a 50 nt 3′ exon.

pHX11 contains the 2.3 kb *Neurospora* mt large rRNA intron and flanking exons cloned downstream of the phage T3 promoter in pBS(+). Linearization of pHX11 with *Ban*I and transcription with phage T3 polymerase yields a 3.2 kb transcript containing an 818 nt 5′ exon, 2.3 kb intron, and 50 nt 3′ exon (Akins & Lambowitz, 1987).

pTyr contains the coding sequence for *Neurospora* mt $tRNA^{Tyr}$ cloned in pUC19, so that linearization with *Bst*NI and transcription with phage T3 RNA polymerase yields a 90 nt transcript corresponding to *Neurospora* mt $tRNA^{Tyr}$ ending with CCA (Guo & Lambowitz, 1992).

p18−1 contains a derivative of the *Neurospora* mt large rRNA intron cloned in pUC18. Linearization of p18-1 with *Kpn*I and transcription with phage T7 RNA polymerase yields a 389 nt transcript corresponding to the excised intron, with the noncoded G-residue at its 5′ end (G. Mohr, A. M. Lambowitz, unpublished).

Synthesis of in Vitro Transcripts. Recombinant plasmids were digested with appropriate restriction enzymes and transcribed with phage T3 or T7 RNA polymerases, using buffers provided by the manufacturers (Stratagene, La Jolla,

CA, and Gibco BRL, Gaithersburg, MD). Transcription reactions were in 100 μL of reaction medium containing 500 μM rNTPs for 60 min at 37 °C. After transcription, the DNA template was digested with 10 units of DNase I (Pharmacia, Piscataway, NJ) for 15 min at 37 °C, and the transcript was extracted twice with phenol−chloroform−isoamyl alcohol (25:24:1; phenol-CIA). ^{32}P-labeled transcripts used in splicing reactions were synthesized by adding 100 μCi of [α-^{32}P]-UTP (3000 Ci/mmol; NEN-DuPont, Boston, MA) to the standard transcription mixture. Higher specific activity ^{32}P-labeled transcripts used in some nitrocellulose-filter-binding experiments were synthesized in reactions with 250 μM each of CTP, GTP, and ATP, plus 50 μM UTP and 150 μCi of [α-^{32}P]UTP (3000 Ci/mmol). pTYR/*Bst*NI was purified by DEAE-Sephacel chromatography, as described (Guo & Lambowitz, 1992). Other transcripts were purified by two cycles of filtration through a G-50 spun column (Pharmacia).

Expression of CYT-18 Protein in E. coli. The CYT-18 protein was synthesized in the E. coli strain BL21(DE3; plysS), which contains a phage T7 RNA polymerase gene under the control of the lac promoter (Rosenberg et al., 1987). Bacteria were transformed with plasmid pEX560, which expresses a wild-type form of the CYT-18 protein (see above), and immediately streaked on LB plates containing 50 μg/mL ampicillin and 12.5 μg/mL chloramphenicol. A single colony from the plates was inoculated into 25 mL of LB medium containing the same antibiotics and grown to OD_{595} = 0.5. At that point, 10% glycerol was added, and 0.1 mL portions of the cells were frozen on dry ice−ethanol and stored at −70 °C. For expression of CYT-18 protein, the frozen cells were thawed and inoculated at 1:10000 dilution into LB medium supplemented with the antibiotics. Each 500 mL of culture was grown in a 4-liter flask shaken at 300 rpm at 30 °C. When the cells reached OD_{595} = 1 (~16 h), 5 mL of 20% lactose was added to induce the synthesis of the CYT-18 protein, and cells were grown for an additional 6 h.

High Salt−PEI Procedure for Purification of CYT-18 Protein. Two liters of *E. coli* cells were chilled on ice and harvested by centrifugation in a Beckman JA-14 rotor (Beckman, Palo Alto, CA) at 3600*g* for 15 min at 4 °C. The cells were resuspended in 20 mL of ice-cold buffer A [25 mM Tris-HCl, pH 7.5, 1 mM EDTA, 10% glycerol, 1 mM dithiothreitol (DTT)] and frozen at −70 °C. Phenylmethanesulfonyl fluoride (PMSF) was added to 0.5 mM, and the frozen pellet was heated at 37 °C until approximately 50% thawed. The cells were then placed on ice and incubated further until lysis was indicated by increased viscosity. All subsequent steps were on ice or at 4 °C. The suspension was diluted 1:5 into 10% glycerol, 25 mM Tris-HCl, pH 7.5, 1 mM EDTA, and 1 mM DTT, and the KCl concentration was adjusted to 400 mM. The suspension was then sonicated using a Branson model 350 sonicator (four bursts, 15 s each at power setting 7), and broken cells were pelleted in a Beckman JA-14 rotor (10 000 rpm, 10 min). Nucleic acids were precipitated from the suspension by adding 10% neutralized polyethyleneimine (PEI) in buffer A containing 5 mM DTT (five 1 mL aliquots, timed 2 min apart), followed by centrifugation in a Beckman JA-14 rotor for 10 min at 10 000 rpm. CYT-18 protein was precipitated from the supernatant with 40% ammonium sulfate, dissolved in 100 mL of buffer A plus 25 mM KCl, and reprecipitated three times with 40% ammonium sulfate to help remove contaminating ribonucleases. The final protein pellet was dissolved in 35 mL of buffer A and dialyzed against two changes of the same buffer (2 h each), after which the dialysate was clarified by centrifugation in a Beckman JA-20 rotor for 10 min at 10 000 rpm.

Carboxymethyl-Sepharose chromatography. Chromatography was at 4 °C in a 30 mL carboxymethyl (CM)-Sepharose column (4.9 cm^2 × 6 cm; Bio-Rad econocolumn with a flow adapter) equilibrated with buffer A. After the sample was applied (35 mL containing 144 mg of protein), the column was washed with two volumes of buffer A and developed with a 250 mL linear gradient of 0−250 mM KCl in buffer A, followed by a final wash with 400 mM KCl in buffer A. The flow rate was 30 mL per h, and 5 mL fractions were collected with a Redifrac fraction collector (Pharmacia). KCl concentrations were measured by using a YSI model 35 conductance meter (YSI Inc., Yellow Springs, OH), calibrated against known concentrations of KCl.

FPLC-Gel Filtration. FPLC-gel filtration was carried out with a Pharmacia LCC501 system controller using a Superose 12 10/30 column (Pharmacia). The column was equilibrated with buffer A containing 250 mM KCl, loaded with a 0.1 mL sample containing 0.2 mg of protein, and run at 0.1 mL/h.

HPLC-Gel Filtration. HPLC-gel filtration was carried out using a Waters 625 LC chromatography system with a Waters Protein Pak 300SW column connected to a Waters 484 tunable absorbance monitor and a Waters 470 scanning fluorescence detector. The column was equilibrated with buffer containing 250 mM KCl, 25 mM Tris-HCl, pH 7.5, and 1 mM EDTA. Samples (20 μL, 32.5 to 10 μM CYT-18 protein) were loaded onto the column, and the column was run at 0.5 mL/h.

Analytical Ultracentrifugation. Analytical ultracentrifugation was carried out in a Beckman model E analytical ultracentrifuge equipped with an electronic speed control, rotor temperature indicator control unit (RTIC), and photoelectric scanner. The protein solution was dialyzed overnight at 4 °C in 200 mM KCl and 25 mM Tris-HCl, pH 7.5, with several buffer changes. For velocity sedimentation experiments, protein samples ranging from 0.02 to 0.2 mg/mL (139 nM to 1.39 μM) were loaded in separate cells that consisted of 12 mm double sector charcoal-filled Epon centerpieces with sapphire windows. The samples were centrifuged at 52 000 rpm at 4 °C in an An-F rotor, and the moving protein boundary was followed by photoelectric scanning at 280 and/or 230 nm at 12 min time intervals. The tracings were recorded by an IBM personal computer as digital data points of concentration distribution as a function of radial distance from the center of rotation.

Sedimentation equilibrium experiments were carried out by the method of Yphantis (1964) in an An-D rotor with double sector charcoal-filled Epon 12 mm centerpieces with sapphire windows. The protein sample was loaded at a concentration of 0.023 mg/mL (159 nM) and centrifuged at 12 000 or 18 000 rpm at 4 °C. The distribution of the protein was monitored by measuring absorbance at 280 and 291 nm with a photoelectric scanner at a series of points across the cell, and baseline correction was made by using absorbance scans at 500 nm. Equilibrium was established by the constancy of the scans over time in hours.

The frictional ratio (f/f_o) was calculated from the measured values for molecular weight and $S°_{20,w}$ by using

$$f/f_o = \frac{M(1 - \bar{\nu}\varrho)}{S^\circ_{20,w}\eta[162\pi^2N^2M(\bar{\nu} + \delta_1\bar{\nu}_1)]^{1/3}}$$

where M is molecular weight of the sedimenting kinetic unit, $\bar{\nu}$ is the protein partial specific volume, 0.735, calculated from its amino acid composition, ϱ is solvent density, η is solvent viscosity, N is Avogadro's number, ν_1 is the specific volume of the solvent, set equal to $\varrho_{H_2O}^{-1}$, and δ_1 is the amount of water associated with the protein in g of H_2O per g of protein (Edsall, 1953). The δ_1 value was estimated by the method of Prakash and Timasheff (1985), with a 30% correction for nonaccessible residues (Hesterberg & Lee, 1981). The value obtained was $\delta_1 = 0.286$.

Tyrosyl Adenylation Assays. Tyrosyl adenylation was assayed in 50 μL of reaction medium containing 0.35 μM CYT-18 protein, 100 mM KCl, 10 mM $MgCl_2$, 144 mM Tris-HCl, pH 7.5, 5 mM ATP, 14 mM β-mercaptoethanol, 10 μCi L-[3,5-^{3}H]tyrosine (40 Ci/mmol; ARC, St. Louis, MO), and 0.1 unit pyrophosphatase (200 units/mg; Boehringer Mannheim, Indianapolis, IN). The reactions were initiated by addition of CYT-18 protein to prewarmed tubes, incubated for 10 min at 30 °C, and then filtered through nitrocellulose filters (Schleicher and Schuell; Keene, NH) to bind the stable CYT-18•tyrosyl adenylate complex. The filters were washed three times with 6 mL of 144 mM Tris-HCl, pH 7.5, 14 mM β-mercaptoethanol, and 10 mM $MgCl_2$, dried, and counted in 10 mL of Ready Protein scintillation cocktail (Beckman), using a Beckman LS1801 scintillation counter.

TyrRS Assays. Unless specified otherwise, TyrRS activity was assayed in 20 μL of reaction medium containing 20–200 nM CYT-18 protein, 100 mM KCl, 15 mM $MgCl_2$, 50 mM Tris-HCl, pH 8.8, 5 mM ATP, 1 μCi of L-[3,5-^{3}H]-tyrosine (40 Ci/mmol; ARC), and 5.8 μM *E. coli* $tRNA^{Tyr}$ (type 2; Subriden, Rolling Bay, WA) or 4.9 μM *Neurospora* mt $tRNA^{Tyr}$ (*in vitro* transcript synthesized from pTYR digested with *Bst*NI). The reactions were initiated by addition of CYT-18 protein to prewarmed tubes, incubated for 6 min at 30 °C, and terminated by addition of 1 mL of 10% TCA and 20 mM sodium pyrophosphate. The precipitated aminoacyl-tRNA was collected by filtration on a glass fiber filter and washed nine times with 3 mL of 2.5% TCA, and 20 mM sodium pyrophosphate. The filters were then dried and counted in 10 mL of Beckman Ready Protein scintillation cocktail, as described above for tyrosyl adenylation assays.

K_m values determined for TyrRS activity assayed in the standard reaction medium at 30°C were as follows: ATP = 0.08 mM, tyrosine = 1.4 μM, *E. coli* $tRNA^{Tyr}$ = 7.1 μM, and *Neurospora* mt $tRNA^{Tyr}$ = 10 μM. The K_m values differed by at most 2-fold when aminoacylation reactions were carried out in splicing reaction medium at 37 °C.

RNA Splicing Assays. RNA splicing was assayed by using ^{32}P-labeled *in vitro* transcript pBD5a/*Ban*I, which contains a 388 nt-derivative of the *Neurospora* mt large rRNA intron that is not self-splicing (Guo et al., 1991). Unless specified otherwise, splicing reactions were in 20 μL of reaction medium containing 100 mM KCl, 5 mM $MgCl_2$, 25 mM Tris-HCl, pH 7.5, 5 mM DTT, 0.5 units of placental RNase inhibitor (United States Biochemical; Cleveland, OH), 1 mM GTP, and amounts of CYT-18 protein indicated in the figures. Reactions were initiated by addition of CYT-18 protein to prewarmed tubes, incubated for the times indicated in the figure legends, and terminated by extraction with phenol-CIA. The aqueous phase was mixed with an equal volume of formamide, 0.01% bromophenol blue, and 0.01% xylene cyanol, and the splicing products were analyzed by electrophoresis in a 6% polyacrylamide/8 M urea gel. After drying the gel, the ^{32}P-labeled RNAs were visualized by autoradiography and quantitated using a Betascope 603 blot analyzer (Betagen; Waltham, MA).

SDS–PAGE. SDS–PAGE was carried out in 0.1% SDS/8% polyacrylamide gels, essentially as described (Laemmli, 1970; Kittle et al., 1991).

Kinetic Measurement of the Rates of Association and Dissociation of CYT-18•RNA Complexes. The rate of association of CYT-18 with the intron-containing RNA was measured by using a Kintek Rapid chemical quenched-flow instrument (Kintek; University Park, PA). After the instrument was equilibrated at 22 or 37 °C, binding reactions were initiated by mixing 15 μL CYT-18 protein at twice the desired final concentration (1–200 nM) with 15 μL ^{32}P-labeled pBD5a/*Ban*I RNA (100 pM) in TMK (10 mM Tris-HCl, pH 7.5, 5 mM $MgCl_2$, 100 mM KCl, 10% glycerol, 5 mM DTT). At various times ranging from 5 ms to 300 s, the sample was mixed with 180 μL of TMK containing 0.5 mg/mL heparin to bind unassociated CYT-18 protein, and the quenched mixture was filtered under gentle vacuum through nitrocellulose (Schleicher and Schuell), backed by DEAE paper (Whatman; Hillsboro, OR). The filters were then washed three times with 1 mL of TMK, dried, and counted separately in 10 mL of Beckman Ready Protein scintillation cocktail, using a Beckman LS1801 scintillation counter. The RNA•protein complexes bind to the nitrocellulose filter, while free RNA binds to the DEAE filter. The simultaneous quantitation of both RNA•protein complexes and free RNA allowed for normalization of the binding data, as described by Wong and Lohman (1993).

To measure the rate of dissociation of CYT-18 protein from the intron RNA, complexes were formed by incubating 10 nM CYT-18 protein dimer with 20 nM ^{32}P-labeled pBD5a/*Ban*I RNA or other RNAs in 1.5 mL of TMK for 30 min at 22 or 37 °C. The complex was then rapidly diluted into 9 mL of TMK or TMK containing 0.5 mg/mL heparin to bind unassociated CYT-18 protein. At different times after the formation of the complex, 1 mL portions were filtered through nitrocellulose under gentle vacuum. The filters were washed three times with 1 mL of TMK, dried, and counted, as above.

Protein Determinations. Protein concentrations were determined either by the dye-binding method (Bradford, 1976), using a Bio-Rad protein assay kit (Bio-Rad, Hercules, CA) with bovine serum albumin as a standard, or by determination of OD_{280}. In the latter case, the extinction coefficient at 280 nm was calculated to be 96 440 M^{-1} cm^{-1} based on an amino acid composition of 12 tryptophans (5690 M^{-1} cm^{-1}) and 22 tyrosines (1280 M^{-1} cm^{-1}) (Edelhoch, 1967; Gill & von Hippel, 1989). Absorbance was measured in 10 M urea, using the same solution as blank. Protein concentrations determined by dye-binding differed by less than 5% from those based on extinction coefficients. Protein concentration determined by absorbance were used in calculating the number of active sites for tyrosyl adenylation or RNA splicing. CYT-18 concentrations are expressed as concentration of dimer throughout.

RESULTS

A New Method for Purifying Bacterially Synthesized CYT-18 Protein. Previous purification protocols for CYT-18 used micrococcal nuclease to free the protein from endogenous nucleic acids prior to fractionation by phosphocellulose or heparin-Sepharose chromatography (Akins & Lambowitz, 1987; Majumder et al., 1989; Kittle et al., 1991). Irrespective of whether the purification was from *Neurospora* mt ribonucleoprotein (RNP) particles or *E. coli*, such columns typically resolved two components of CYT-18 protein, one bound to the column and the other in the column flow through. The former was active in splicing and aminoacylation, whereas the latter had a decreased ratio of splicing to TyrRS activity (Akins & Lambowitz, 1987; Majumder et al., 1989; Kittle et al., 1991).

We recognized that the two chromatographically resolved forms of CYT-18 might reflect the incomplete removal of nucleic acids. To overcome this difficulty, we devised a new purification method in which nucleic acids were precipitated from *E. coli* lysates by using polyethyleneimine (PEI), a procedure shown to effectively remove nucleic acids from restriction enzymes and other nucleic acid-binding proteins (Burgess, 1991). After PEI precipitation of nucleic acids, the CYT-18 protein was purified from the supernatant by ammonium sulfate fractionation and chromatography in a CM-Sepharose column. CM-Sepharose was substituted for heparin-Sepharose used previously (Kittle et al., 1991) to reduce the expense of purifying large amounts of CYT-18 protein.

Figure 1 shows the CM-Sepharose column profile from a purification of wild-type CYT-18 protein synthesized in *E. coli* from the T7 promoter-driven expression plasmid, pEX560 (see Materials and Methods). Column fractions were assayed for TyrRS activity by using *E. coli* $tRNA^{Tyr}$ and for splicing activity by using ^{32}P-labeled *in vitro* transcript pBD5a/*Ban*I, which contains a 388 nt "mini"-derivative of the *Neurospora* mt large rRNA intron (Guo et al., 1991). This intron is completely dependent on the CYT-18 protein for *in vitro* splicing and was used as the standard group I intron RNA substrate in the present work. Proteins in column fractions were analyzed by SDS−PAGE. The chromatogram shows that all of the CYT-18 protein bound to the column and eluted at 170−190 mM KCl in a single peak having both TyrRS activity and splicing activity. In other experiments, the *E. coli*-synthesized CYT-18 protein prepared by the PEI method eluted from heparin-Sepharose columns as a single peak at 0.5 M KCl, under conditions that previously gave two distinct peaks of the protein (G. Mohr and A. M. Lambowitz, unpublished data). Likewise, CYT-18 protein isolated from *Neurospora* mt RNP particles by PEI precipitation bound quantitatively and eluted as a single peak from a CM-Sepharose column (not shown). We infer that the two peaks of CYT-18 protein observed previously were due to incomplete removal of nucleic acids.

Table 1 summarizes the purification of the *E. coli*-synthesized CYT-18 protein via the PEI-precipitation procedure, and Figure 2 shows the purity of the protein at the various steps. In the experiment shown, CYT-18 was recovered after CM-Sepharose chromatography at approximately 60% yield and 89% purity. In other experiments, the yields ranged from 60 to 70% and purities ranged from 90 to 95% (not shown). In all cases, the major contaminants

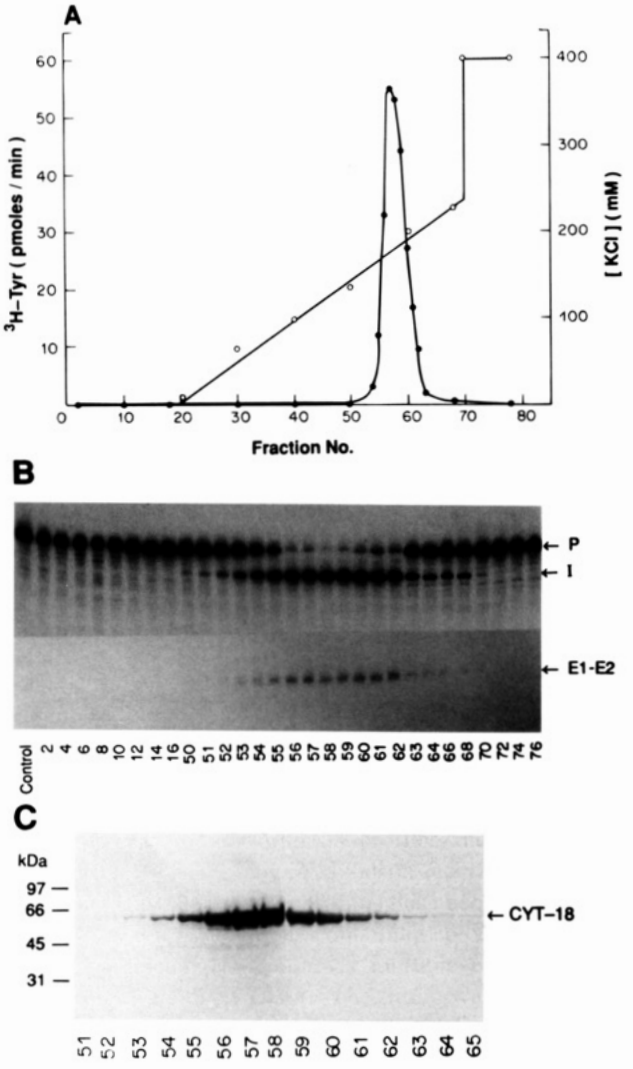

FIGURE 1: CM-Sepharose chromatography of CYT-18 protein synthesized in *E. coli*. CYT-18 protein synthesized from plasmid pEX560 in *E. coli* strain BL21(DE3; pLysS) was isolated by PEI precipitation and ammonium sulfate fractionation, followed by chromatography in a 30 mL CM-Sepharose column, as described in Materials and Methods. The column was eluted with a linear gradient of 0−250 mM KCl in buffer A and then washed with 400 mM KCl in buffer A. (A) TyrRS assays. TyrRS activity was assayed in 2 μL portions of column fractions, as described in Materials and Methods. When necessary, column fractions were diluted to less than 50 μg protein/mL to ensure the assay was not saturated. KCl concentrations of column fractions were determined by conductivity. (B) Splicing assays. Splicing activity was assayed in 2 μL portions of column fractions, by using a ^{32}P *in vitro* transcript pBD5a/*Ban*I, which contains a 388 nt derivative of the *Neurospora* mt large rRNA intron. The control lane shows unreacted ^{32}P-labeled *in vitro* transcript incubated under the same conditions, but in the in the absence of added protein. Products of splicing reactions were analyzed by electrophoresis in a 6% polyacrylamide/8 M urea gel, followed by autoradiography of the dried gel. (C) SDS−PAGE analysis of proteins in column fractions. Proteins in 2.5 μL portions of column fractions were analyzed by electrophoresis in a 0.1% SDS/8% polyacrylamide gel, which was stained with Coomassie blue. Numbers at the left indicate sizes (kDa) and positions of Bio-Rad low molecular weight marker proteins run in the same gel. Abbreviations: E1−E2, ligated exons 1 and 2; I, excised intron; P, precursor RNA.

after the CM-Sepharose step were smaller proteins that cross-react with anti-CYT-18 antibody. These smaller proteins most likely result from inefficient initiation of translation at downstream AUGs, since they are present in cells lysed by addition of boiling sample buffer and their sizes decreased

Table 1: Purification of CYT-18 Protein Synthesized in *E. coli*[a]

fraction	volume (mL)	protein conc. (mg/mL)	total protein (mg)	purity (%)	yield (%)
lysate	100	9.4	936	11	100
PEI-supernatant	100	7.3	728	15	100
$(NH_4)_2SO_4$ ppt	100	1.5	148	52	73
dialysate	35	4.1	144	54	73
CM-Sepharose	45	1.6	70	89	60

[a] CYT-18 was purified by PEI precipitation of nucleic acids, $(NH_4)_2SO_4$ fractionation, and chromatography in a CM-Sepharose column, as described in Materials and Methods. Protein concentrations were measured by the method of Bradford (1976), using a Bio-Rad protein assay kit, and purity was estimated by densitometry of the Coomassie blue-stained SDS−polyacrylamide gel shown in Figure 2. The table shows total protein, the yield of CYT-18 protein, and its purity at each stage of the purification.

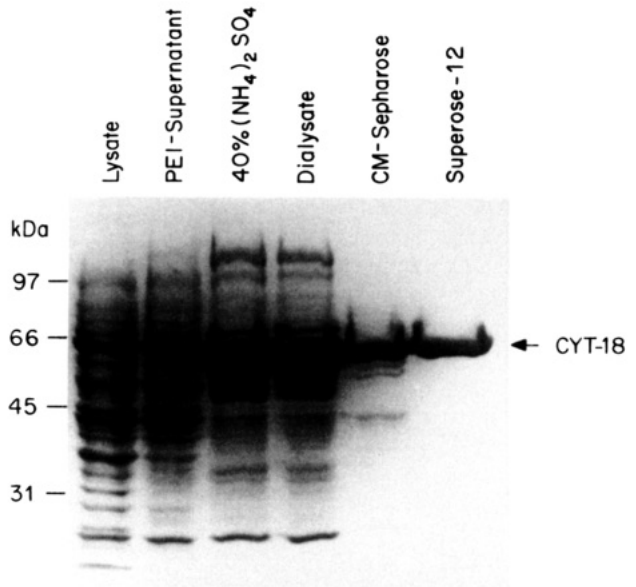

FIGURE 2: SDS−PAGE of the CYT-18 preparation at different stages of purification. Fractions were analyzed by electrophoresis in a 0.1% SDS/8% polyacrylamide gel, which was stained with Coomassie blue. Fractions prior to the CM-Sepharose column contained 25 μg of protein measured by Bradford assays. The CM-Sepharose fraction (fraction 58 from the column of Figure 1) and the Superose 12-fraction each contained 5 μg of protein. The numbers at the left indicate sizes (kDa) and positions of the Bio-Rad low molecular weight marker proteins run in the same gel.

in parallel with that of the major CYT-18 protein band when synthesized from expression plasmids having C-terminal truncations (not shown). CYT-18 protein at a purity >99% could be obtained by a final FPLC-gel filtration through Superose-12 (Figure 2). As long as freezing was avoided, essentially 100% of the CYT-18 protein remained active in binding the group I intron-containing RNA, as judged by nitrocellulose-filter-binding assays (not shown). The protein was stable when stored on ice for 4−6 months.

HPLC-Gel Filtration and Glycerol Gradient Centrifugation. The relatively pure preparations of CYT-18 from *E. coli* were used to investigate the quaternary structure of the protein in solution. Initial HPLC-gel filtration and glycerol gradient centrifugation experiments suggested that CYT-18 protein might have an unusually elongated shape. The MW of the CYT-18 protein calculated from its amino acid composition is 72 158. In HPLC-gel filtration, CYT-18 protein at concentrations from 62.5 nM to 1 μM eluted as a single major peak at a position corresponding to a globular protein of 280 kDa, equivalent to a tetramer. By contrast, in glycerol gradients, TyrRS and splicing activity cosedimented with the major peak of CYT-18 protein at a position corresponding to a globular protein of 66 kDa, equivalent to a monomer. The results of the HPLC gel filtration and glycerol gradient centrifugation could be reconciled by assuming that CYT-18 protein is a dimer having an elongated shape.

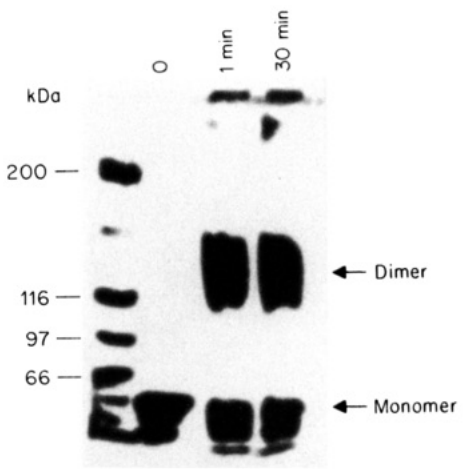

FIGURE 3: Cross-linking of CYT-18 protein with dimethyl suberimidate. CYT-18 protein (7.2 μg) in 100 μL of 100 mM KCl, 5 mM $MgCl_2$, 50 mM triethanolamine-HCl, pH 8.2, and 5 mM DTT was incubated with 3 mg/mL dimethyl suberimidate (Sigma) for 1 or 30 min at 22 °C. The reaction was terminated by addition of 10 μL of 1 M glycine, and the products were analyzed by electrophoresis in a 0.1% SDS/5% polyacrylamide gel, which was stained with Coomasie blue. Prior to cross-linking, CYT-18 monomers migrate at a molecular mass of 64 kDa. The major cross-linked species migrates at a molecular mass of 128 kDa, expected for a CYT-18 homodimer.

Chemical Cross-Linking. Direct evidence that CYT-18 is a homodimer was obtained by experiments in which the protein was incubated with the chemical cross-linker dimethyl suberimidate and then analyzed by SDS−PAGE. As shown in Figure 3, CYT-18 incubated in the absence of cross-linker migrated at a position corresponding to a molecular mass of 64 kDa, as expected for a monomer, whereas incubation with the cross-linker for 1 or 30 min resulted in a predominant band at a molecular mass of 128 kDa, as expected for a homodimer. The cross-linking was rapid and efficient, with no significant conversion of the dimer to higher molecular weight species after longer cross-linking times. The same result was obtained when CYT-18 was cross-linked in the presence of a group I intron RNA substrate (500 nM pBD5a/*Ban*I RNA; not shown).

Analytical Ultracentrifugation. To conclusively determine the quaternary structure of the CYT-18 protein and obtain further information about its shape, we performed analytical ultracentrifugation. In initial velocity sedimentation experiments, CYT-18 protein ranging in concentration from 0.02 to 0.2 mg/mL (139 nM to 1.39 μM) was sedimented at 52 000 rpm in an analytical ultracentrifuge. Photoelectric scanning at various wavelengths showed that the protein sedimented as a single boundary during the entire experiment, indicating that the preparation is homogenous. At the protein concentrations tested, there was no significant dependence of $S_{20,W}$ on protein concentration, and the extrapolation to zero protein concentration gave $S^\circ_{20,W} = 5.45$ (Figure 4).

In sedimentation equilibrium experiments, CYT-18 protein at a loading concentration of 0.023 mg/mL (159 nM) was

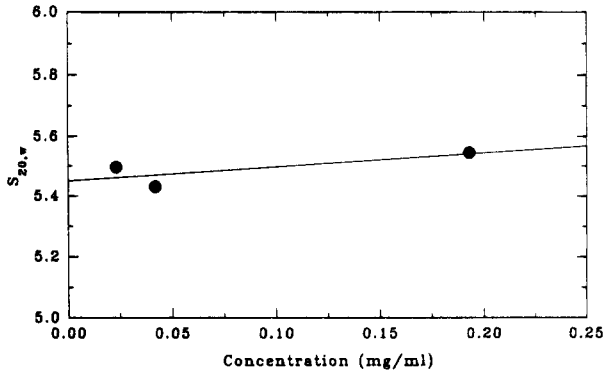

FIGURE 4: Velocity sedimentation of CYT-18 protein. Protein samples ranging from 0.02 to 0.2 mg/mL were sedimented in 200 mM KCl and 25 mM Tris-HCl, pH 7.5 at 4 °C, as described in Materials and Methods. The figure shows $S_{20,w}$ as a function of CYT-18 protein concentration. The line was drawn by first-order regression fitting of the data points.

sedimented at two different speeds (12 000 or 18 000 rpm) until equilibrium was attained. Similar results were obtained at both centrifugation speeds. As shown in Figure 5 for the experiment at 18 000 rpm, the protein distribution at equilibrium was plotted as a function of half the square of radial distance, and two data sets obtained by monitoring protein concentration at 280 and 291 nm were simultaneously fitted to different models by the Nonlin program (Johnson et al., 1981). Figure 5 panels A and B show that the data are consistent with either a nonassociating solution with a fixed molecular mass of 144 kDa, corresponding to that of a CYT-18 dimer (nonideality coefficient = 0.058), or with an associating ideal solution in which the smallest associating species has the molecular mass of a CYT-18 monomer and a $K_{dim} \geq 1.44 \times 10^7\ M^{-1}$ (nonideality coefficient = 0.031). Since the dimerization constant is high, the two models are indistinguishable, and we infer that the protein exists in solution as a dimer.

From the experimentally determined molecular weight and the $S°_{20,w}$, the shape of the protein can be visualized by calculating its frictional ratio (f/f_o) and axial ratio (a/b), as described in Materials and Methods. The calculated value for f/f_o is 1.55, corresponding to an axial ratio of 10 for a prolate ellipsoid of revolution and 12 for an oblate ellipsoid (Svedberg & Pedersen, 1940). Thus, the protein is asymmetric, as inferred from its behavior in HPLC-gel filtration and glycerol gradient centrifugation.

Determination of the Number of Active Sites for Tyrosyl Adenylation. Studies with bacterial TyrRSs have shown that the number of active sites for tyrosyl adenylation can be determined by measuring the stoichiometry of protein-bound tyrosyl adenylate complex, since the complex is stable and tyrosyl adenylation is irreversible in the presence of pyrophosphatase (Fersht et al., 1975; Wilkinson et al., 1983). Similar determinations of CYT-18-linked tyrosyl adenylate formed per homodimer for four different CYT-18 preparations gave values ranging from 0.8 to 1.5 with a mean of 1.2 ± 0.3. These values suggest that CYT-18, like the bacterial TyrRSs (Jakes & Fersht, 1975), contains one active site for tyrosyl adenylation per CYT-18 protein dimer.

The Splicing Activity of the CYT-18 Protein Is Not Affected by Substrates of the Aminoacylation Reaction. To investigate whether the splicing activity of the CYT-18 protein might be influenced by the aminoacylation reaction, we carried out

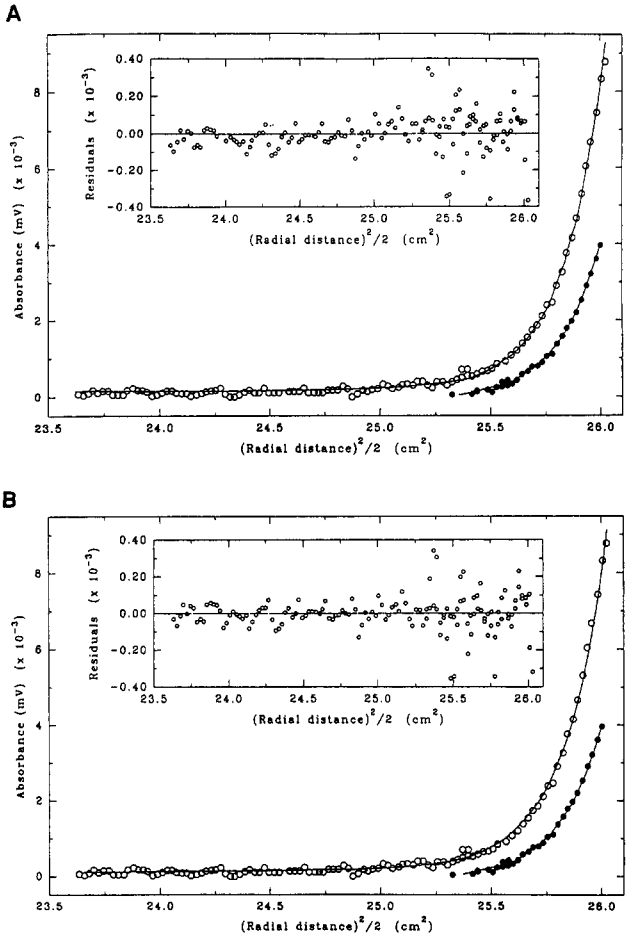

FIGURE 5: Equilibrium sedimentation analysis of CYT-18 protein. CYT-18 protein (0.023 mg/mL) in 200 mM KCl and 25 mM Tris-HCl, pH 7.5 was sedimented at 18 000 rpm at 4 °C. The position of the protein was monitored by scanning the absorbance at 280 and 291 nm until equilibrium was attained, as judged by no change in position as a function of time in hours. The equilibrium distribution of the protein, determined from the data obtained at 280 (○) and 291 nm (●), is plotted against half of the square of the radial distance. In panel A, the lines show the best simultaneous fit of the two data sets to the nonassociating model. In panel B, the lines show the best simultaneous fit of the two data sets to a model of CYT-18 monomers associating to dimers with an association constant of $\geq 1.44 \times 10^7\ M^{-1}$. The insets show the residuals of the fitting.

in vitro splicing reactions in the presence of different aminoacylation substrates. The reactions were carried out with 0.1 μM CYT-18 protein and 0.5 μM ^{32}P-labeled pBD5a/*Ban*I precursor RNA at both high (1 mM) and low (20 μM) GTP concentrations. Under both sets of conditions, the rate of splicing was unaffected by tyrosine, ATP, *E. coli* $tRNA^{Tyr}$, or *Neurospora* mt $tRNA^{Tyr}$ at concentrations ordinarily used in the aminoacylation reaction (1 mM ATP, 1 mM tyrosine, 5.8 μM of *E. coli* $tRNA^{Tyr}$, and 4.9 μM *Neurospora* mt $tRNA^{Tyr}$; not shown). It made no difference whether these substrates were added alone or in different combinations to support tyrosyl adenylation or aminoacylation by CYT-18.

The TyrRS Activity of the CYT-18 Protein Is Inhibited by GTP or Other Ribonucleotides. By contrast to the lack of effect of aminoacylation substrates on splicing, we found that the TyrRS activity of the CYT-18 protein was strongly inhibited by the splicing cofactor GTP at concentrations in the mM range (Table 2). Additional experiments showed that CYT-18's TyrRS activity was also inhibited by CTP or

Table 2: The TyrRS Activity of CYT-18 Protein Is Inhibited by GTP and Other Ribonucleotides[a]

conditions	[^{3}H]Tyr incorporated (cpm)
CYT-18	
control (ATP)	131095 (±3800
+GTP	29442 (±3369)
+UTP	17791 (±246)
+CTP	585 (±70)
E. coli TyrRS	
control (ATP)	23661 (±192)
+GTP	31262 (±174)
+UTP	34605 (±485)
+CTP	21237 (±395)

[a] TyrRS activity was assayed using [^{3}H]tyrosine and *E. coli* tRNA^{Tyr}, as described in Materials and Methods, except that the reactions contained 0.125 mM ATP plus 7.5 mM of the NTP being tested. *E. coli* TyrRS activity was assayed using a commercial aminoacyl-tRNA synthetase preparation (Sigma A3646; Sigma, St. Louis, MO). Assays were performed in duplicate with the variance indicated in parentheses.

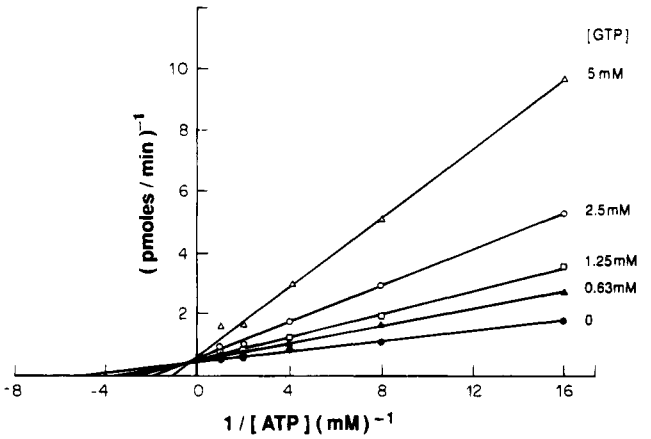

FIGURE 6: Competitive inhibition of TyrRS activity by GTP. Aminoacylation reactions were carried out in 20 μL of reaction medium containing 5.8 μM *E. coli* tRNA^{Tyr}, 1 μCi of L-[3,5-^{3}H]-tyrosine (40 Ci/mmol), 110 nM CYT-18 protein, and varying amounts of GTP (0−5 mM) and ATP (0.0625−1 mM). Reactions were initiated by addition of CYT-18 to prewarmed tubes, incubated for two min at 30 °C, and terminated by adding 1 mL of 10% TCA and 20 mM sodium pyrophosphate. The reciprocal velocity of the aminoacylation reaction, measured by the production of the charged tRNA, is plotted against the reciprocal of the ATP concentration. The K_i was determined from a replot of the inhibitor concentrations against the slopes of the lines in the reciprocal plot.

UTP, with the order of inhibition CTP ≫ UTP > GTP. Interestingly, the *E. coli* TyrRS was found to be insensitive to the same concentrations of GTP or the other ribonucleotides (Table 2).

To determine the nature of the inhibition of CYT-18 by GTP, TyrRS activity was measured while covarying ATP from 0.0625 to 1 mM and GTP from 0 to 5 mM. A Lineweaver-Burke plot of the data showed that the inhibition is competitive with respect to ATP, and that GTP has a K_i = 0.86 mM, approximately four times the K_m value for ATP in this experiment (0.19 mM; Figure 6). A repeat of the experiment gave a K_i^{GTP} = 1.0 mM (not shown). In other experiments, we found that 5 mM GTP did not support aminoacylation of *E. coli* tRNA^{Tyr} by the CYT-18 protein and that guanosine, which is also used efficiently as a splicing cofactor (K_m = 14 μM; Kittle et al., 1991), had no effect on CYT-18's TyrRS activity when added at concentrations up to its solubility limit (approximately 2 mM; not shown). Together, these findings indicate that GTP competes non-productively with ATP for the nucleotide-binding site of the CYT-18 protein. The relatively poor ability of CYT-18 to discriminate between ATP and other ribonucleotides could be relevant to its regulation *in vivo* (see Discussion).

The TyrRS Activity of CYT-18 Is Inhibited by a Group I Intron RNA. We previously reported that the binding of group I intron RNAs to the CYT-18 protein is substantially stronger than is the binding of tRNA^{Tyr} and that the pBD5a/*Ban*I RNA, which contains the 388 nt derivative of the Neurospora mt large rRNA intron, competitively inhibits the aminoacylation of *E. coli* tRNA^{Tyr} (Guo & Lambowitz, 1992). In the present work, we extended these findings to show that pBD5a/*Ban*I RNA also inhibits aminoacylation of the Neurospora mt tRNA^{Tyr} and that, for both tRNAs, it makes no difference whether the intron RNA is added before or after the initiation of the aminoacylation reaction (not shown). Assuming comparable concentrations of substrates and the absence of other regulatory mechanisms, these findings indicate that splicing should occur preferentially to aminoacylation in vivo.

Kinetic Measurements of the Association and Dissociation of CYT-18·Intron RNA Complexes. The rate of association of CYT-18 protein with the group I intron RNA substrate RNA was measured by using a rapid chemical quenched-flow apparatus. CYT-18 protein at concentrations ranging from 1 to 200 nM was mixed with 50 pM ^{32}P-labeled pBD5a/*Ban*I RNA. After various times, further binding was quenched by adding 0.5 mg/mL heparin, and the formation of heparin-resistant CYT-18·RNA complexes was assayed by retention on nitrocellulose filters. We confirmed that the amount of heparin added was sufficient to completely block new complex formation, without promoting the dissociation of existing complexes (see k_{off} measurements; Figure 8 below).

Figure 7 panels A and B show representative binding data obtained at 22 and 37 °C, respectively. At 37 °C, the temperature at which splicing is assayed, the binding data obtained at all protein concentrations were best fitted to an equation with two exponentials ($A_1e^{-k_1t} + A_2e^{-k_2t}$, where A_1 and A_2 are the amplitudes and k_1 and k_2 are the rate constants of the first and second phases, respectively). As shown in Figure 7D, the rate of the first phase at 37 °C increased linearly with CYT-18 protein concentration, as expected for a bimolecular association. From the slope of the line, we calculate that the bimolecular association rate constant (k_{on}) = 3.24 ± 0.03 × 10^7 M^{-1} s^{-1}. By contrast, Figure 7E shows that the rate of the second phase at 37 °C did not increase linearly with CYT-18 concentration, and the data were best fitted to a hyperbola with a maximum rate constant of 0.54 ± 0.07 s^{-1}. This maximum rate constant was confirmed by an additional experiment using 1 μM CYT-18 (not shown). At 22 °C, the binding at 50 and 200 nM CYT-18 was biphasic, but the two phases were not well resolved at lower protein concentrations. Consequently, the rates for the first exponential at 50 and 200 nM CYT-18 were plotted together with those for the single exponential at 1 and 5 nM CYT-18. Figure 7C shows that the association rate at 22 °C also increases linearly with CYT-18 protein concentration, with the slope of the line yielding a k_{on} of (4.12 ± 0.17) × 10^7 M^{-1} s^{-1}. The rate constant of the slower phase at 200 nM CYT-18 at 22 °C was 0.47 s^{-1} (not shown), close to the maximum rate constant of 0.54 s^{-1} for this phase at 37 °C.

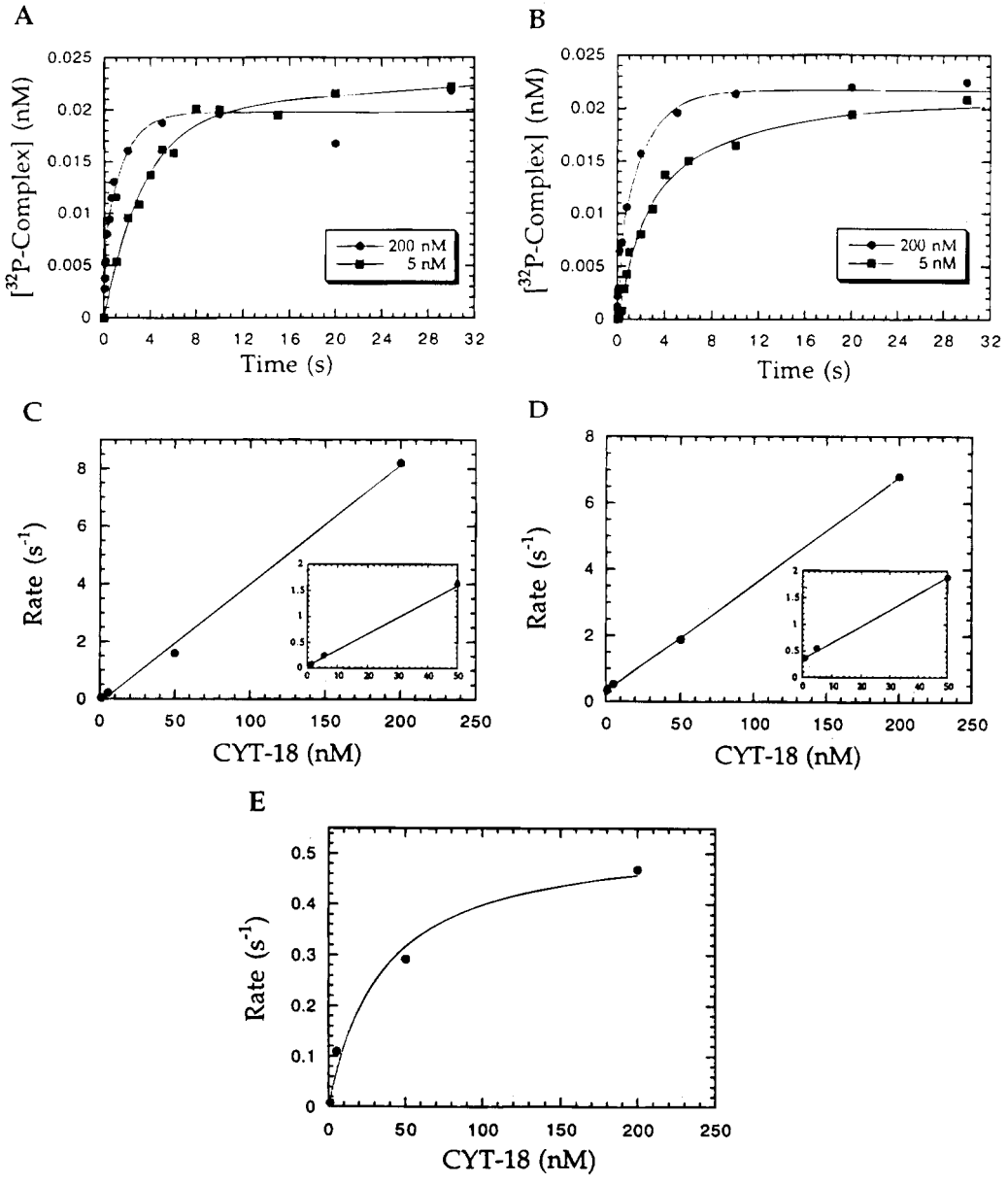

FIGURE 7: Kinetic measurement of the rates of association of CYT-18 protein with a group I intron-containing RNA. The rate of complex formation was measured by using a Kintek rapid chemical quenched-flow instrument equilibrated at 22 or 37°C. For each time point, 15 μL of CYT-18 protein (2−400 nM in TMK) was mixed with an equal volume of 100 pM ^{32}P-labeled pBD5a/*Ban*I RNA in TMK buffer to achieve a final concentration of 50 pM RNA and 1−200 nM CYT-18. At the indicated times, the reaction was quenched with 0.18 mL of TMK containing 0.5 mg/mL heparin, to bind any free CYT-18 protein, and immediately filtered through nitrocellulose. Panels A and B show representative binding data from experiments at 22 and 37 °C, respectively, using 5 (■) or 200 (●) nM CYT-18 protein. Panels C and D show the rate of the first phase of complex formation as a function of CYT-18 concentration at 22 and 37 °C, respectively. The k_{on}s calculated from the slopes of the lines are 4.12 ± 0.17 × 10^7 M^{-1} s^{-1} at 22 °C and 3.24 ± 0.03 × 10^7 M^{-1} s^{-1}. The insets show the data at low protein concentrations plotted on an expanded scale. (E) The rate of the second phase of CYT-18 complex formation at 37 °C as a function of CYT-18 concentration. The data are best fitted to a hyperbola saturating at 0.54 ± 0.07 s^{-1}.

Significantly, we detected no lag in CYT-18 binding to the intron RNA, even at very low protein concentrations (0.5 nM; not shown), indicating that any step required prior to binding, such as the dimerization of CYT-18 from inactive monomers, is not rate limiting.

The pattern of a linear rate increase followed by hyperbolic rate increase with increasing protein concentration is consistent with a two-step association process in which the initial binding of CYT-18 is followed by a slower conformational change. The biphasic kinetics are unlikely to reflect the binding of CYT-18 to two RNA conformational isomers, since in that case we expect two bimolecular association processes with different rate constants. Although it remains possible that only a subpopulation of the group I intron substrates requires the CYT-18-dependent conformational change to form a tight complex, we observed the same biphasic binding at 37 °C, irrespective of whether the RNA was heated to 90 °C and slowly cooled prior to binding (not shown).

To measure the dissociation rate of CYT-18·RNA complexes, the complexes were formed for 30 min by mixing 20 nM of ^{32}P-labeled RNA and 10 nM CYT-18 protein dimer and then diluted 10-fold and challenged with 0.5 mg/mL heparin, which was sufficient to quench all binding when added prior to complex formation (Figure 8, arrow marked by asterisk). Remarkably, the complexes between the CYT-

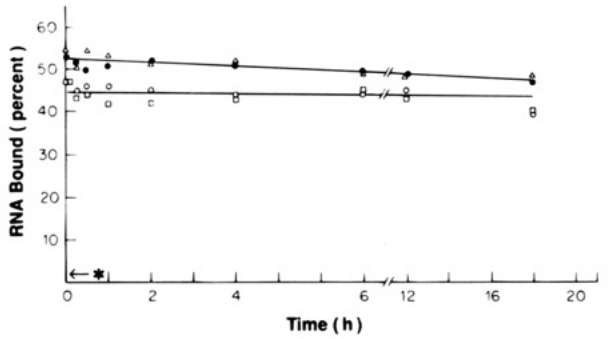

FIGURE 8: Kinetics of dissociation of the CYT-18·intron RNA complexes. Complexes were formed by incubating 10 nM CYT-18 protein dimer with 20 nM ^{32}P-labeled transcript pBD5a/*Ban*I (precursor RNA) or p18-1/*Kpn*I (excised intron RNA) in 1 mL of TMK for 30 min at 22 °C. At the indicated times, the complex was diluted into 9 mL of TMK (Δ, pBD5a/*Ban*I; ○, p18−1/*Kpn*I) or TMK containing 0.5 mg/mL heparin to trap dissociated CYT-18 protein (●, pBD5a/*Ban*I; □, p18-1/*Kpn*I) and immediately filtered through nitrocellulose. The figure plots the amount of complex retained on the filter as a function of time. The arrow marked by an asterisk shows that binding was abolished when 0.5 mg/mL heparin was added prior to formation of the complex. The k_{off} determination using pBD5a/*Ban*I RNA was repeated four times with similar results. In some of these experiments, a small proportion (<20%) of the complex dissociated in the first 10 min, with the majority of the complex remaining stable for at least 16 h.

18 protein and *in vitro* transcripts corresponding to unspliced precursor RNA (pBD5a/*Ban*I) or the excised intron RNA (p18-1/*Kpn*I) showed minimal dissociation over 18 h (Figure 8). In other experiments, the rate of dissociation of CYT-18 from either the precursor or excised intron RNA was not substantially increased by KCl up to 250 mM, 1 mM ATP, or ATP + Tyr + *E. coli* tRNA^{Tyr} or *Neurospora* mt tRNA^{Tyr} at concentrations used in aminoacylation reactions (not shown).

The K_d value for the CYT-18·intron RNA complex, calculated from the ratio of k_{off} over k_{on} at 22 or 37 °C, was <0.3 pM. This value is substantially lower than that determined by presumed equilibrium binding experiments, which gave a K_d of 6 nM for the complex between CYT-18 and pBD5a/*Ban*I RNA (Guo & Lambowitz, 1992). For *in vitro* transcript pHX11/*Ban*I, which contains the full-length 2.3 kb mt large rRNA intron, k_{off} and k_{on} measurements at 22 °C gave a K_d = 22 pM (not shown), still very tight binding.

Kinetic Analysis of the Splicing Reaction. In view of the tight binding of CYT-18 to the intron RNA, the kinetics of the splicing reaction were measured under pre-steady-state conditions. Figure 9A shows an experiment in which splicing reactions were carried out with CYT-18 protein dimer at concentrations of 101, 146, and 219 nM and a 2−4-fold excess of in vitro transcript pBD5a/*Ban*I precursor RNA (438 nM). Each of the reactions showed an initial burst of splicing, whose amplitude was approximately equal to the amount of CYT-18 protein dimer added, followed by a plateau in which little if any further splicing occurred. The lack of turnover presumably reflects the very tight binding of CYT-18 protein to the excised intron RNA (see above). Controls showed that virtually all of the RNA substrate could be spliced when excess CYT-18 protein was added and that all of the CYT-18 protein in the preparation was active in binding the pBD5a/*Ban*I RNA in nitrocellulose-filter-binding

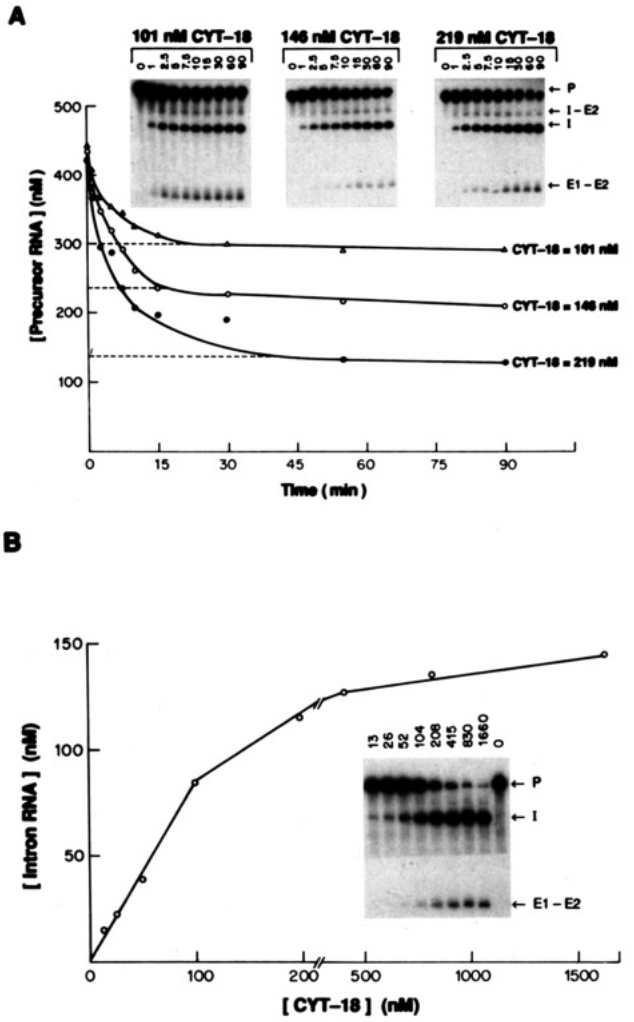

FIGURE 9: Kinetics and stoichiometry of the CYT-18 protein-dependent splicing reaction. In panel A, splicing reactions were carried out in 200 μL of reaction medium containing 459 nM ^{32}P-labeled pBD5a/*Ban*I RNA (40 105 cpm/pmol) and 101, 146, or 219 nM CYT-18 protein dimer, as described in Materials and Methods. Reactions were initiated by addition of CYT-18 protein and incubated at 37 °C. At the times indicated, 25 μL portions were withdrawn, and the reaction was terminated by rapid mixing with an equal volume of phenol-CIA. Splicing products were analyzed by electrophoresis in 6% polyacrylamide/8 M urea gels, followed by autoradiography of the dried gels and quantitation with a Betagen betascope 603 blot analyzer. The figure shows a plot of the disappearance of precursor RNA as a function of time, with the insets showing autoradiograms of the dried gels. In panel B, splicing reactions were in 25 μL of reaction medium containing 146 nM ^{32}P-labeled pBD5a/*Ban*I RNA (13 840 cpm/pmol) and 13−1660 nM CYT-18 protein. The reactions were initiated by addition of CYT-18 protein and incubated for 60 min at 37 °C and then terminated and analyzed by electrophoresis in a 6% polyacrylamide/8 M urea gel, as above. The figure shows a plot of the appearance of excised intron RNA as a function of CYT-18 protein concentration, with the inset showing an autoradiogram of the dried gel. The experiment was repeated with similar results.

assays (not shown). In addition, we confirmed that the CYT-18 protein was not inactivated when incubated for 120 min under the same conditions, but in the absence of added substrate (not shown). The rate constant for splicing calculated from the data in Figure 9 was 0.0025 s^{-1}, within 6-fold of that for self-splicing of the Tetrahymena large rRNA intron in vitro (0.015 s^{-1} or 0.91 min^{-1}; Cech & Bass, 1986).

To confirm that there is one active site for splicing per CYT-18 protein dimer and that the protein does not turn over,

we carried out splicing reactions using a constant amount (146 nM) of pBD5a/*Ban*I precursor RNA and increasing amounts of CYT-18 protein. The reactions were incubated for 60 min, a relatively long time which should be sufficient for multiple rounds of catalysis. As shown in Figure 9B, the amount of excised intron RNA produced in each reaction was roughly equal to the amount of CYT-18 protein dimer, up to at least 100 nM CYT-18 protein. If CYT-18 were capable of turning over, the amount of intron spliced should exceed the amount of CYT-18 protein added at these concentrations. Consistent with the hypothesis that CYT-18 is sequestered by binding to the intron RNA, we confirmed that micrococcal nuclease digestion of the RNAs after the 60 min splicing reaction led to release of CYT-18 protein, which could then utilize fresh substrate (not shown).

DISCUSSION

In the present work, we developed a new procedure for purifying highly active, bacterially expressed CYT-18 protein via PEI precipitation to remove tightly bound nucleic acids. Unlike previous purification protocols which gave two chromatographically distinct forms of the CYT-18 protein from either *E. coli* or from *Neurospora* mt RNP particles (Akins & Lambowitz, 1987; Majumder et al., 1989; Kittle et al., 1991), the new procedure gives CYT-18 protein that elutes from CM-Sepharose or heparin-Sepharose columns as a single peak with substantially increased yield. We infer that the two peaks of CYT-18 observed previously were due to incomplete removal of nucleic acids, not covalent modification of the protein.

By using analytical ultracentrifugation and other physical methods, we show that CYT-18 exists in solution as a homodimer having an elongated shape. The measured frictional ratio, $f/f_o = 1.55$, corresponds to an axial ratio of 10 for a prolate ellipsoid or 12 for an oblate ellipsoid. By comparison, f/f_o values for globular proteins typically range from 1.1 to 1.2 (axial ratios = 2−5), whereas fibrinogen, an elongated molecule, exhibits an $f/f_o = 2.3$ (axial ratio = 31; Tanford, 1961). The elongated shape of the CYT-18 protein results in anomalous hydrodynamic behavior not exhibited by the *Bacillus stearothermophilus* TyrRS (Jones et al., 1985) and likely reflects the presence of additional sequences at both the N- and C-termini of CYT-18 (Cherniack et al., 1990).

Like bacterial TyrRSs, the CYT-18 protein exhibit half-sites reactivity, each homodimer having only one active site for tyrosyl adenylation and RNA splicing. It has been suggested that half-sites reactivity of the bacterial TyrRSs reflects the fact that a relatively elongated tRNA cannot be accommodated by a relatively small-sized monomer protein and must instead bind asymmetrically across the surface of the two subunits of the homodimer (Ward & Fersht, 1988). The presence of only one active site for splicing per CYT-18 protein dimer suggests that the intron RNA also binds across both subunits of the homodimer, consistent with the previous conclusion that the binding site for the intron overlaps that for $tRNA^{Tyr}$. The elongated shape of the CYT-18 protein may be an adaptation that contributes to its function in RNA splicing by providing a larger surface with which the intron can interact.

Experiments examining possible regulatory mechanisms showed that the splicing activity of the CYT-18 protein was unaffected by aminoacylation substrates ATP, tyrosine, and *E. coli* or *Neurospora* mt $tRNA^{Tyr}$, at concentrations that support tyrosyl adenylation or aminoacylation, whereas the TyrRS activity was inhibited by splicing cofactor GTP or other ribonucleotides. The measured K_i for GTP, 0.86 mM, is within the range of intracellular GTP concentrations in bacterial or mammalian cells (0.92 and 0.48 mM, respectively; Kornberg & Baker, 1992), suggesting that the observed inhibition may be physiologically significant. The finding that aminoacylation is inhibited by GTP, but not by guanosine, presumably reflects the fact that the protein makes relatively strong contacts with the phosphate groups of the nucleotide, as has been inferred for the binding of ATP by the homologous bacterial TyrRSs (Brick et al., 1988). The *E. coli* TyrRS is not inhibited by similar concentrations of GTP or other nucleotides and presumably has some structural difference in the nucleotide-binding cleft, which renders it more specific for ATP.

$$E + R \underset{}{\overset{3.2 \times 10^7}{\rightleftharpoons}} ER \underset{< 0.00001}{\overset{0.54}{\rightleftharpoons}} ER' \overset{0.0025}{\rightleftharpoons} EP \overset{< 0.00001}{\rightleftharpoons} E + P$$

FIGURE 10: Minimal reaction scheme for CYT-18-dependent splicing of a group I intron. At 37 °C, the binding of CYT-18 to the group I intron RNA substrate occurs with a bimolecular rate constant of $(3.24 \pm 0.03) \times 10^7$ M^{-1} s^{-1}, followed by a slower step, likely a conformational change, having a rate constant of 0.54 $\pm$ 0.07 s^{-1}. After binding, splicing proceeds at 0.0025 s^{-1}. Under *in vitro* conditions, the CYT-18 protein is limited to one round of catalysis due to its extremely slow dissociation from the excised intron RNA (<0.00001 s^{-1}).

Kinetic analysis of the splicing of the 388 nt version of the *Neurospora* mt large rRNA intron by the CYT-18 protein is consistent with the minimal reaction scheme shown in Figure 10. The binding of the CYT-18 protein is biphasic, consistent with a two-step process in which an initial bimolecular association step whose rate is close to diffusion-limited ($3.24 \pm 0.03 \times 10^7$ M^{-1} s^{-1}) is followed by a slower step (0.54 $\pm$ 0.07 s^{-1}). In principle, this slow step could be a conformational change in either the CYT-18 protein or the intron RNA that allows the formation of a tight complex. Chemical structure mapping of CYT-18-dependent group I intron RNAs has shown that most of the conserved group I intron secondary structure can form in the absence of CYT-18 protein, but that CYT-18 is required for formation of the active tertiary structure (Mohr et al., 1994; Caprara et al., manuscript in preparation.) Thus, the biphasic binding observed here might reflect rapid binding of CYT-18 to the unfolded intron, followed by all or part of a slower conformational change leading to the active tertiary structure. Our data do not distinguish whether all or only a subpopulation of the RNA must undergo a conformational change to form a tight complex, and this same qualification would also apply if the biphasic binding were due to a protein conformational change.

Following binding, the splicing of the intron proceeds with a rate constant of 0.0025 s^{-1}, within 6-fold of the rate constant for self-splicing of the *Tetrahymena* large rRNA intron (0.015 s^{-1} or 0.91 min^{-1}; Cech & Bass, 1986). Kinetic analysis of reactions in which the L-21 version of the *Tetrahymena* ribozyme cleaves a separate RNA molecule containing the 5′ splice site showed that the rate constant for the chemical cleavage step is 5.8 s^{-1} (Herschlag & Cech, 1990). The slower rate of splicing of the *Tetrahymena* intron

($0.015\ s^{-1}$) has been taken to suggest that the rate-limiting step is an unspecified conformational change required for the 5′ cleavage reaction to proceed in the intact precursor RNA. For the *Neurospora* intron, the relatively slow rate of splicing following CYT-18 binding may reflect the same rate-limiting step as in the *Tetrahymena* splicing reaction or some other slow conformational change that distinguishes the protein-assisted reaction. Subsequent turnovers in the CYT-18-dependent reaction are limited by the rate of dissociation of CYT-18 protein from the excised intron RNA.

The K_d for the complex between CYT-18 protein and its group I intron RNA substrate, measured by determining k_{off} and k_{on}, was <0.3 pM at 22 or 37 °C, substantially lower than the K_d value of 6 nM from presumed equilibrium binding experiments (Guo & Lambowitz, 1992). Such tight binding is not readily measured by equilibrium methods because of the very long time periods required to attain equilibrium at very low protein and RNA concentrations and because very low concentrations of CYT-18 may dissociate into inactive monomers or be lost by nonspecific adsorption to tubes. In addition, the previous equilibrium-binding experiments were carried out in the presence of nonspecific competitor RNA, which effectively lowered the amount of free CYT-18 protein. In work that will be described elsewhere, we have remeasured by kinetic methods the K_ds for other group I introns and for different segments of the *Neurospora* mt large rRNA intron that were determined previously (Guo & Lambowitz, 1992). The results showed that the previous conclusions are qualitatively correct, but that K_d values were in most cases overestimated due to the problems indicated above. The remeasured K_d values reinforce the previous conclusion that binding of the intron RNA to the CYT-18 protein (K_d <0.3 pM) is substantially stronger than is the binding of $tRNA^{Tyr}$ [K_d = 10 μM as estimated from K_m; see discussion in Guo and Lambowitz (1992)]. The difference in K_ds for the two RNA substrates corresponds to a difference in binding energy of at least −10.2 kcal/mol. As discussed previously, the much tighter binding of the intron could reflect additional contacts with the protein or that binding of the tRNA is accompanied by an energetically unfavorable conformational change (Guo & Lambowitz, 1992). The binding of the CYT-18 protein to group I intron RNA appears to be among the strongest RNA·protein interaction recorded. By comparison, the K_d for the interaction of the R17 coat protein with its binding site is 1 nM (Carey & Uhlenbeck, 1983), the K_d for the TFIIIA·5S RNA complex is 0.7 nM (Romanuick, 1985), and the K_d for U1A·U1 snRNA complex is 20 pM (Hall & Stump, 1992).

Finally, the finding that the CYT-18 protein functions stoichiometrically in *in vitro* splicing reactions due to its extremely slow dissociation from the intron RNA suggests that specific mechanisms may be required to promote dissociation of the protein from the excised intron *in vivo*. Such mechanisms could include modification of the CYT-18 protein to decrease its affinity for intron RNA, endo- or exonucleolytic degradation of the excised intron RNA, or the action of other proteins, such as RNA helicases, which have been suggested to facilitate the release of spliced mRNAs from spliceosomes (Company et al., 1991; Guthrie, 1991). The existence of components that degrade excised group I intron RNAs is suggested by the findings that mutations in the nuclear genes *cyt-4* in *Neurospora* and *suv3* in yeast lead to the accumulation of excised group I intron RNAs in mitochondria (Garriga et al., 1984; Dobinson et al., 1989; Conrad-Webb et al., 1990). The yeast *suv3* gene encodes a protein having similarity to RNA helicases and may dissociate group I intron-splicing complexes, prior to their degradation (Stepien et al., 1992). The *Neurospora cyt-4* gene encodes a protein having amino acid sequence similarity to the *Saccharomyces cerevisiae* SSD1/SRK1 protein and *Schizosaccharomyces pombe* DIS3 protein, which have been implicated in the function of cell cycle protein phosphatases (Turcq et al., 1992), and to *E. coli* RNase II, whose sequence was recently added to the data base (G. Mohr, The Ohio State University, and I. Saira Mian, University of California, Santa Cruz, personal communications). Thus, either the CYT-4 protein may regulate intron degradation via protein phosphorylation or it may function directly in degrading excised intron RNAs. Interestingly, quantitation showed that the amount of group I intron RNAs that accumulate in the *Neurospora cyt-4-1* mutant is sufficient to bind a significant proportion (at least 75%) of the CYT-18 protein (R. Saldanha and A. M. Lambowitz, unpublished data). This finding raises the intriguing possibility that mutant strains with primary defects in RNA turnover could have secondary defects in RNA splicing and protein synthesis resulting from sequestration of CYT-18 protein in complexes with excised group I intron RNAs.

ACKNOWLEDGMENT

We thank Ms. Janet Gianelos for the CYT-18 protein preparations used in some of the experiments, Dr. Daniel Herschlag (Stanford University) for helpful discussions and suggesting the experiment in Figure 9B, and Drs. Mark Caprara, Georg Mohr and Sabine Mohr for their comments on the manuscript.

REFERENCES

Akins, R. A., & Lambowitz, A. M. (1987) *Cell 50*, 331−345.
Bedouelle, H. (1990) *Biochimie 72*, 589−598.
Bedouelle, H., & Winter, G. (1986) *Nature 320*, 371−373.
Bradford, M. M. (1976) *Anal. Biochem. 72*, 248−254.
Brick, P., Bhat, T. N., & Blow, D. M. (1988) *J. Mol. Biol. 208*, 83−98.
Burgess, R. R. (1991) *Methods Enzymol. 208*, 3−10.
Carey, J., & Uhlenbeck, O. C. (1983) *Biochemistry 22*, 2610−2615.
Carter, P., Bedouelle, H., & Winter, G. (1986) *Proc. Natl. Acad. Sci. U.S.A. 83*, 1189−1192.
Cech, T. R., & Bass, B. L. (1986) *Annu. Rev. Biochem. 55*, 599−629.
Cherniack, A. D., Garriga, G., Kittle, J. D., Jr., Akins, R. A., & Lambowitz, A. M. (1990) *Cell* 62, 745−755.
Collins, R. A., & Lambowitz, A. M. (1985) *J. Mol. Biol. 184*, 413−428.
Company, M., Arenas, J., & Abelson, J. (1991) *Nature 349*, 487−493.
Conrad-Webb, H., Perlman, P. S., Zhu, H., & Butow, R. A. (1990) *Nucleic Acids Res. 18*, 1369−1376.
Dessen, P., Zaccai, G., & Blanquet, S. (1982) *J. Mol. Biol. 159*, 651−664.
Dobinson, K. F., Henderson, M., Kelley, R. L., Collins, R. A., & Lambowitz, A. M. (1989) Genetics 123, 97−108.
Edelhoch, H. (1967) *Biochemistry 6*, 1948−1954.
Edsall, J. T. (1953) in *The Proteins* (Neurath, H., & Bailey, K., Eds.) Vol. 1B, pp 549−726, Academic Press, New York.
Fersht, A. R. (1975) *Biochemistry 14*, 5−12.
Fersht, A. R., Ashford, J. S., Bruton, C. J., Jakes, R., Koch, G. L. E., & Hantley, G. S. (1975) *Biochemistry 14*, 1−4.
Garriga, G., & Lambowitz, A. M. (1983) *J. Biol. Chem. 258*, 14745−14748.
Garriga, G., & Lambowitz. A. M. (1986) *Cell 46*, 669−680.

Garriga, G., Bertrand, H., & Lambowitz, A. M. (1984) *Cell 36*, 623−634.
Gill, S. C., & von Hippel, P. (1989) *Anal. Biochem. 182*, 319−326.
Guo, Q., & Lambowitz, A. M. (1992) *Genes Dev. 6*, 1357−1372.
Guo, Q., Akins, R. A., Garriga, G., & Lambowitz, A. M. (1991) *J. Biol. Chem. 266*, 1809−1819.
Guthrie, C. (1991) *Science 253*, 157−163.
Hall, K. B., & Stump, W. T. (1992) *Nucleic Acids Res. 20*, 4283−4290.
Herschlag, D., & Cech, T. R. (1990) *Biochemistry 29*, 10159−10171.
Hesterberg, L. K., & Lee, J. C. (1981) *J. Biol. Chem. 256*, 9724−9730.
Jakes, R., & Fersht, A. R. (1975) *Biochemistry 14*, 3344−3350.
Johnson, M. L., Correia, J. J., Yphantis, D. A., & Halvorson, H. R. (1981) *Biophys. J. 36*, 575−588.
Jones, D. H., McMillan, A. J., & Fersht, A. R. (1985) *Biochemistry 24*, 5852−5857.
Kämper, U., Kück, U., Cherniack, A. D., & Lambowitz, A. M. (1992) *Mol. Cell. Biol. 12*, 499−511.
Kim, S. H., & Cech, T. R. (1987) *Proc. Natl. Acad. Sci. U.S.A. 84*, 8788−8792.
Kittle, J. D., Jr., Mohr, G., Gianelos, J. A., Wang, H., & Lambowitz, A. M. (1991) *Genes Dev. 5*, 1009−1021.
Kornberg, A., & Baker, T. A. (1992) *DNA Replication*, 2nd ed., Freeman, New York.
Laemmli, U. K. (1970) *Nature 227*, 680−685.
Majumder, A. L., Akins, R. A., Wilkinson, J. G., Kelley, R. L., Snook, A. J., & Lambowitz, A. M. (1989) *Mol. Cell. Biol. 9*, 2089−2104.
Michel, F., & Westhof, E. (1990) *J. Mol. Biol. 216*, 585−610.
Mohr, G., Zhang, A., Gianelos, J. A., Belfort, M., & Lambowitz, A. M. (1992) *Cell 69*, 483−494.
Mohr, G., Caprara, M. G., Guo, Q., & Lambowitz, A. M. (1994) *Nature 370*, 147−150.
Prakash, V., & Timasheff, S. N. (1985) *Methods Enzymol. 117*, 53−60.
Romanuick, P. J. (1985) *Nucleic Acids Res. 13*, 5369−5387.
Rosenberg, A. H., Lade, B. N., Chui, D. S., Lin, S. W., Dunn, J. J., & Studier, F. W. (1987) *Gene* 56, 125−135.
Stepien, P. P., Margossian, S. P., Landsman, D., & Butow, R. A. (1992) *Proc. Natl. Acad. Sci. U.S.A. 89*, 6813−6817.
Svedberg, T., & Pedersen, K. O. (1940) *The Ultracentrifuge*, Clarendon Press, Oxford.
Tanford, C. (1961) *Physical Chemistry of Macromolecules*, pp 358−359, John Wiley and Sons, Inc., New York.
Turcq, B., Dobinson, K. F., Serizawa, N., & Lambowitz, A. M. (1992) *Proc. Natl. Acad. Sci. U.S.A. 89*, 1676−1680.
Ward, W. H. J., & Fersht, A. R. (1988) *Biochemistry 27*, 5525−5530.
Wilkinson, A. J., Fersht, A. R., Blow, D. M., & Winter, G. (1983) *Biochemistry 22*, 3581−3586.
Wong, I., & Lohman, T. M. (1993) *Proc. Natl. Acad. Sci. U.S.A. 90*, 5428−5432.
Yphantis, D. A. (1964) *Biochemistry 3*, 297−317.

BI941699M